

The effect of temperature on the sealability of bismuth–tin alloy plugs

Lewaa Hmadeh^{*}, Marcelo Anunciação Jaculli, Noralf Vedvik, Behzad Elahifar, Sigbjørn Sangesland

Norwegian University of Science and Technology, Department of Geoscience and Petroleum, Trondheim, Norway

ARTICLE INFO

Keywords:

Plugging and abandonment
Sealability
Bismuth alloy plugs
Push-out test
Temperature
Numerical simulation model

ABSTRACT

Innovative solutions for plugging oil and gas wells are becoming increasingly important to ensure safe operations, save costs, and guarantee that the wells are sealed with a long-term perspective. Among these innovations, bismuth alloys have emerged as a potential sealing material, attracting attention for their distinctive properties. Despite the promising characteristics of bismuth alloys, comprehensive testing is required to fully understand their behavior and to validate their suitability as a sealing barrier. This study focuses on testing the sealability of eutectic bismuth–tin alloy plugs across a range of temperatures (23–120 °C). Examining this influence is crucial because bismuth alloys can be engineered to have specific melting points and characteristics, allowing them to respond effectively to the prevailing temperature conditions in the wellbore. To this end, the study employs an integrated approach, combining laboratory experiments and numerical simulations, to assess the performance of the plug under the influence of the variables pressure, temperature, and curing time through push-out tests. Preliminary results indicate that the sealing efficiency of the bismuth–tin alloy tends to increase over time at lower temperatures, whereas it decreases significantly as temperatures approach its melting point. Therefore, the eutectic bismuth–tin alloy can be employed safely as an environmental plug, but its applicability as a deep-set plug in high-temperature wells is questioned. In this case, selecting an alloy that has a higher melting point is recommended. This work not only underscores the necessity of understanding the thermodynamic influences on bismuth alloys but also sets the stage for future innovations in well sealing technologies, potentially establishing new industry standards.

1. Introduction

Bismuth–tin (BiSn) metal plugs have gained much attention in the last couple of years, proving to be a suitable replacement for Portland cement plugs and a path to a safe, cost-effective, environmentally friendly plugging and abandonment (P&A) operations. This alloy stands out among other alternative materials due to its unique properties. The BiSn metal alloy has a relatively low melting point (138 °C) compared to other metals, has a viscosity similar to that of water when melted, is very dense with a specific gravity (SG) of 10, tends to expand upon solidification, is non-corrosive, non-toxic and resistant to H₂S and CO₂, and importantly it is a eutectic metal, meaning that it goes from liquid to solid phase instantly during the solidification process, thus circumventing the gel phase (Carragher and Fulks, 2018; Knutsen, 2019; Stoll, 2017).

Laboratory tests have investigated the bonding between bismuth alloys and steel pipe (Hmadeh et al., 2023a; (Hmadeh et al., 2023b),

(Hmadeh et al., 2024b); (Manataki et al., 2023) and between bismuth alloys and rock formation samples (Zhang et al., 2020; (Zhang et al., 2021), (Zhang et al., 2022)), indicating that bismuth plugs display higher bond strength than cement plugs in the A-annulus (bonded to steel) and B-annulus (bonded to the formation). In addition, bismuth plugs displayed lower leakage flow rates due to being impermeable, leaving the micro-annulus formed between the plug and the steel pipe as the only possible leak path. It is important to highlight that bismuth–tin alloys do not bond with a steel casing; instead, their ability to adhere to the casing and withstand mechanical and hydraulic loads relies solely on their expansion coupled with the friction at the plug–pipe interface, resulting in a “hydraulic shear bond strength”. This hydraulic shear bond strength could be influenced by several factors such as the plug material, surface roughness, viscosity of the pressuring fluid, curing conditions (curing pressure, temperature, and time). In addition, internal temperature and pressure variations could initiate a radial debonding along the radial interface between the pipe and the plug,

^{*} Corresponding author

E-mail address: lewaahmadeh@ntnu.no (L. Hmadeh).

<https://doi.org/10.1016/j.geoen.2024.213107>

Received 7 March 2024; Received in revised form 24 April 2024; Accepted 6 July 2024

Available online 10 July 2024

2949-8910/© 2024 The Authors. Published by Elsevier B.V. This is an open access article under the CC BY license (<http://creativecommons.org/licenses/by/4.0/>).

consequently leading to a seal failure (Carter and Evans, 1964; Yang et al., 2020).

So far, bismuth alloy plugs primarily found applications as environmental surface plugs as part of their initial testing phase. This alloy has also been employed in diverse well applications such as multi-annulus isolation, water shut-off through gravel pack screens, and isolation of sustained casing pressure (Fulks et al., 2021). However, the prospect of utilizing bismuth alloys for deep plugging and high-temperature well applications remains a subject of ongoing investigations. This hesitancy within the industry arises from the limited knowledge regarding the behavior of the material at elevated temperatures, as bismuth alloys possess a relatively low melting point, posing constraints on its widespread application and qualification as a potential alternative to cement plugs. Grasping how temperature influences the sealing performance of the plug allows for the creation of a tailored and secure seal. This understanding enhances the success of P&A operations in the oil and gas sector, ensuring compliance with safety and environmental regulations.

Operating close to the melting temperature of a bismuth alloy plug primarily leads to the emergence of a major concern: creep. Creep refers to the gradual deformation of materials subjected to sustained loads over time and exacerbated by operating temperatures close to the melting point. In P&A, creep can be a major concern for sealing materials (e.g., cement, mechanical plugs) and other well barrier elements due to its effect on the long-term integrity of such elements, especially the well plug. Various sealing materials may therefore experience deformation due to factors like temperature, pressure, and/or stresses from the surrounding formation. Creep effects become more evident with elevated temperatures, which could pose a problem for bismuth alloy plugs deployed in surrounding temperatures approaching their melting point. It is also worth emphasizing that creep may occur even when the stress levels are below the yield strength, and this can happen due to prolonged exposure to stress. Furthermore, aging effects become relevant with the combined effects of high temperature, high loads, and extended periods of time, effectively degrading elastic properties, which may compromise the sealability of metal alloy plugs.

Hence, the primary aim of this study is to investigate how different temperatures impact the performance of plugs made of the eutectic bismuth-tin alloy. This is a continuation of previous studies we carried out in our research group (Hmadeh et al., 2023a; (Hmadeh et al., 2023b), (Hmadeh et al., 2024b)), in which the effect of temperature had not been verified yet. Examining this influence is crucial because bismuth alloys can be engineered to have specific melting points and characteristics, allowing them to respond effectively to the prevailing temperature conditions in the wellbore. Laboratory tests and numerical simulations are carried out to capture the performance of this plug under the influence of the variables pressure, temperature, and curing time through push-out tests. Results indicate that the sealing capability of this alloy improves over time at lower temperatures but decreases significantly at temperatures closer to its melting point. Therefore, the eutectic bismuth-tin alloy can be employed safely as an environmental plug, but its applicability as a deep-set plug in high-temperature wells is questioned. In this case, selecting an alloy that has a higher melting point is recommended. However, its behavior concerning creep resistance would require further examination.

2. Methodology

2.1. Materials used

The materials used are similar to the ones adopted in previous studies (Hmadeh et al., 2023a; (Hmadeh et al., 2023b)). In this section, some parts are repeated for convenience, while the changes are noted.

The primary materials of relevance are bismuth-tin alloy blocks, Portland G cement, steel X-52 pipe, and casting sand. Detailed properties of the listed materials are presented. The chosen low-melting-point alloy

was “MCP 137” composed of 58% bismuth and 42% tin (5N Inc, 2012), which is referred to as the eutectic metal alloy. The properties of the eutectic bismuth-tin alloy can be found in Table 1, with further details about its elastic properties as a function of temperature seen in Table 2. Properties of bismuth-tin alloys are available in the literature in several works as previously collected by Hmadeh et al. (2024a).

The selection of the X-52 steel pipe (Rolf Lycke AS, 2012) was based on its similar characteristics to those of casings and tubings utilized in offshore settings, coupled with the inaccessibility of actual casing pipes. The pipes were cut into 250 mm long sections with an inner diameter (ID) of 53.35 mm and an outer diameter (OD) of 60.80 mm. Its properties are provided in Table 3.

The casting sand, above which the alloy plugs are poured, is oil-based and finely grained. Hence, when well compacted, the sand prevents the molten bismuth alloy from seeping toward the bottom outlet of the test cell. The “test cell” is a collective term that refers to an X-52 metal pipe in which a bismuth plug is set, a steel cap fixed at each end of the pipe, and four bolts. To maintain a secure seal and hold the assembly together even under high pressures, bolts positioned along the sides of the pipe pass through the edges of both caps and are then tightened using eight steel nuts from either end of the cell.

All pipes used in this study were filled with 95 mm of casting sand, above which a 121 mm bismuth alloy plug was set. A 34 mm gap (above the plug) was left empty for experimental purposes as shown in Fig. 1. This pipe-plug setup is the very same setup adapted in our previous research products (Hmadeh et al., 2023a; (Hmadeh et al., 2023b); (Hmadeh et al., 2024b)) and was preferred to be kept as is for the sake of data consistency and ease of data comparison.

2.2. Experimental setup

A small-scale laboratory setup was used to conduct this study. The setup includes two VP-12K Vindum Engineering hydraulic pumps connected to two “test-cells” placed in an electric oven. The Vindum hydraulic pump is equipped with two side-by-side cylinders that manage to pump water continuously exerting a shear force on top of the plug. The configuration of the utilized setup is illustrated in Fig. 2.

The black wires immersed in the beaker are responsible for the water intake. The steel rod, on which a valve and a pressure monitor are mounted and connected to the top of the test cell, serves as the water outlet. The test cells feature a bottom outlet that can be opened or closed depending on the specific test being performed.

2.3. Experimental procedure

The experiments conducted in this study can be divided into two

Table 1
Properties of the eutectic BiSn alloy.

| Property | Eutectic bismuth-tin alloy (Bi58–Sn42) |
|--|--|
| Density | 8.56 ~ 8.73 g/cm ³ |
| Young’s modulus | 42.72 ~ 43 GPa |
| Poisson’s ratio | 0.3426 |
| Yield strength | 50 ~ 70 MPa |
| Ultimate strength | 70 ~ 80 MPa |
| Melting point | 135 ~ 139°C |
| Coefficient of thermal expansion | 15 ~ 17 μm/(m·°C) @ 20 ~ 90°C |
| Linear expansion after casting (observed at 20 °C) | 0.015% @ 1 hour 0.03% @ 3 hours 0.045% @ 8 hours 0.06% @ 1 day 0.07% @ 3 days 0.08% @ 10 days 0.09% @ 1 month 0.095% @ 3 months 0.1% @ 12 months |

Table 2

Elastic properties as a function of temperature for the eutectic bismuth-tin alloy.

| Temperature [°C] | Bulk modulus [GPa] | Shear modulus [GPa] |
|------------------|--------------------|---------------------|
| 20 | 43.186 | 16.449 |
| 30 | 43.040 | 16.315 |
| 40 | 42.895 | 16.181 |
| 50 | 42.750 | 16.034 |
| 60 | 42.605 | 15.859 |
| 70 | 42.460 | 15.672 |
| 80 | 42.314 | 15.484 |
| 90 | 42.169 | 15.255 |
| 95 | 42.097 | 15.107 |
| 100 | 42.024 | 14.953 |
| 105 | 41.951 | 14.784 |
| 110 | 41.879 | 14.593 |
| 115 | 41.806 | 14.401 |
| 120 | 41.734 | 14.195 |
| 125 | 41.661 | 13.990 |
| 127.5 | 41.625 | 13.842 |
| 130 | 41.588 | 13.643 |
| 132.5 | 41.552 | 13.325 |
| 135 | 41.516 | 12.822 |

Table 3

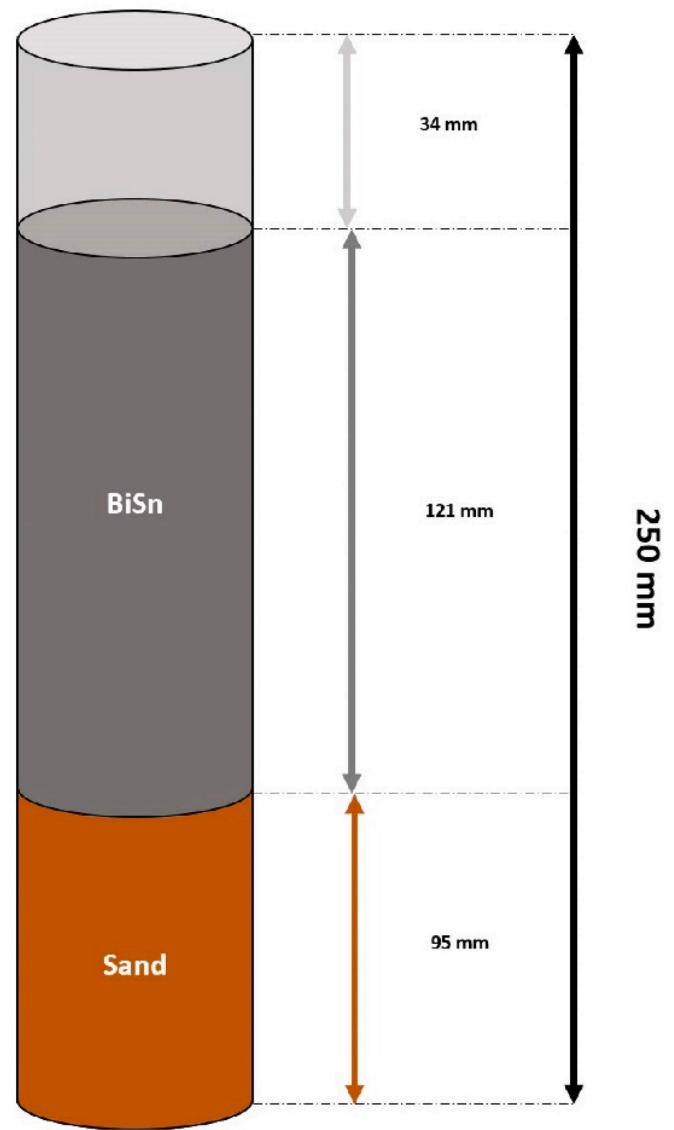
Properties of the steel X-52.

| Property | Steel X-52 |
|----------------------------------|------------------------|
| Density | 7.84 g/cm ³ |
| Young's modulus | 212 GPa @ 20°C |
| | 207 GPa @ 100°C |
| | 200 GPa @ 200°C |
| | 193 GPa @ 300°C |
| | 185 GPa @ 400°C |
| Poisson's ratio | 176 GPa @ 500°C |
| | 0.284 @ 20°C |
| | 0.287 @ 100°C |
| | 0.291 @ 200°C |
| | 0.295 @ 300°C |
| Yield strength | 0.299 @ 400°C |
| | 0.303 @ 500°C |
| | 358 MPa |
| | 500 MPa |
| | 12 μm/(m°C) @ 20°C |
| Coefficient of thermal expansion | 12 μm/(m°C) @ 100°C |
| | 13 μm/(m°C) @ 200°C |
| | 13 μm/(m°C) @ 300°C |
| | 14 μm/(m°C) @ 400°C |
| | 14 μm/(m°C) @ 500°C |

phases: a preparatory phase and a testing phase. The preparatory stage starts with a bismuth plug set in a pipe as conveyed in Fig. 1 and allowed to cool down at standard conditions. The pipes are then secured in the test cells (Fig. 2), and a pressure of 40 bara is applied by setting the hydraulic pump on PPBD mode (Paired Pressure Bi-Directional). This mode allows the pumps to continuously deliver fluid (in our case, water) to reach a constant pressure of 40 bara, with a fluid flow rate adjusted automatically by the pump to maintain this set pressure. The choice of 40 bara as the pressure setting is intended to prevent water from evaporating during the melting process. This decision is based on a previous study (Hmadeh et al., 2023b) that showed a better plug sealing performance under 40 bara pressure compared to higher pressures.

The next step is locking the pipes in the test cells and exerting pressure of 40 bara by setting the hydraulic pump on PPBD mode where the pump will deliver fluid (water in our case) continuously at a set constant pressure (40 bara). The fluid flow rate varies to maintain the set pressure. A pressure of 40 bara was chosen to prevent water from evaporating during the melting process. Based on a previous study conducted (Hmadeh et al., 2023a), it was witnessed that the plug setup in use showed better performance under 40 bara compared to higher or lower pressures.

After maintaining the pressure constant, the electric oven is switched

**Fig. 1.** Pipe-plug setup.

on to 185 °C. The temperature chosen is high enough to melt the bismuth plug set in place and falls within the temperature capacity of the O-rings used. Around 2 h into the melting process, pressure and flow rate fluctuations are witnessed signaling the start of the plug melting inside the pipe. The pump then manages to stabilize the pressure, and the plug is left in the oven for 2 extra hours to ensure the full melting of the plug. In total, it requires approximately 4 h to achieve complete melting of the plug.

After plug melting is ensured, the pressure is left constant, and the heater is lowered to multiple temperatures that fall below the melting point of the alloy. It is important to mention that all tested samples were furnace-cooled meaning that slow annealing took place. All samples were kept in the furnace, at a defined temperature and 40 bara of pressure, for several hours which we refer to as curing time. Curing time was recorded from the moment the temperature was reduced. The chosen experimental parameters are listed in Table 4. This marks the end of the preparatory phase.

The testing phase starts with depleting the trapped pressure below the plug by opening the bottom outlet of the test cell 24 h before testing; except for the test carried out after 24 h of curing, the bottom outlet is opened 12 h before testing. Upon opening, some water starts flowing out, which was expected since during the melting process of the plug,

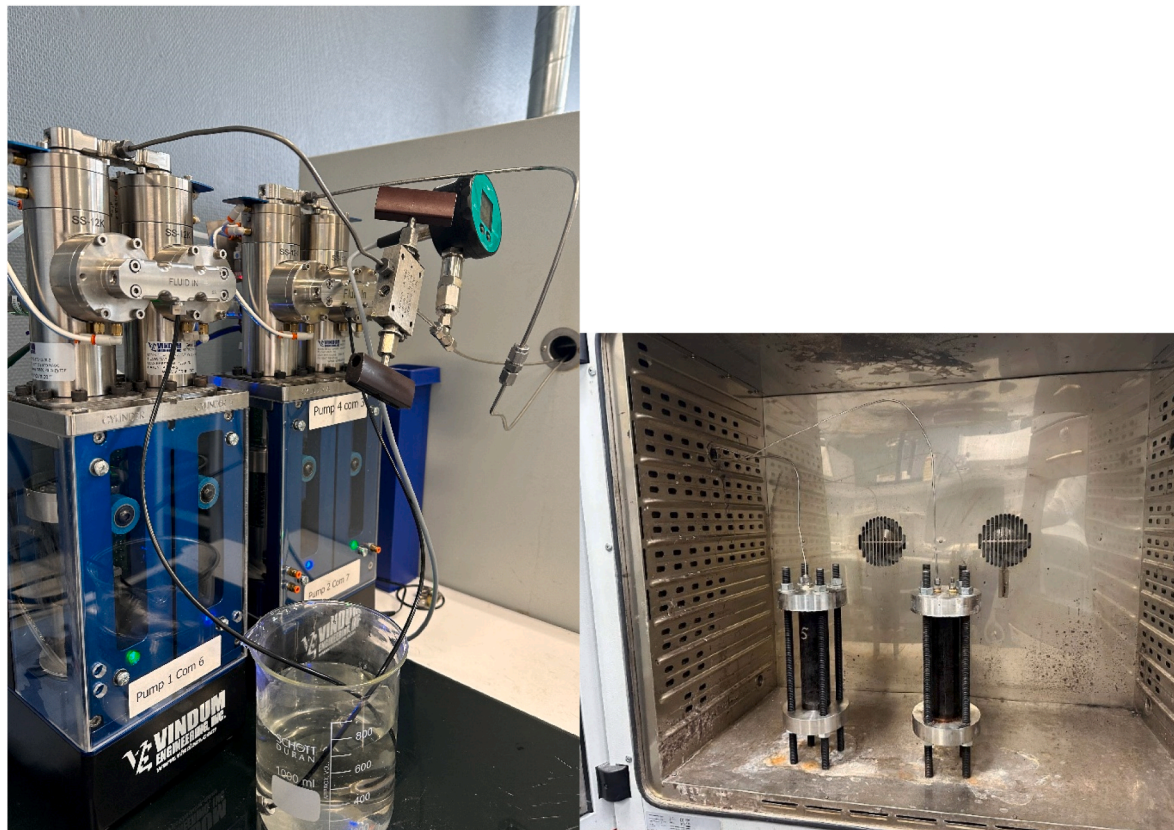


Fig. 2. Test setup Configuration: Hydraulic pumps (left) and test cells in an electric oven (Right).

Table 4
Experimental parameters.

| Curing Temperatures ($^{\circ}\text{C}$) | Curing time (hours) |
|--|---------------------|
| 23, 40, 60, 70, 80, 90, 120 | 24, 48, 72, 96 |

water starts to bypass the molten alloy filling up the sand underneath. Until the testing time begins, the pressure on top of the plug remains constant (40 bara) indicating that the plug is intact and no leakage through the plug-pipe interface has yet occurred. To start testing, the PPBD pump mode is stopped and immediately switched to PRD mode (Paired Rate Delivery) in which the pump will deliver fluid continuously at a set constant rate - in our case 0.4 ml/min. The aim here is to increase the pressure on top of the plug starting from 40 bara (setting pressure) until it hydraulically fails, indicating the creation of micro-annuli along the pipe-plug interface. The test is stopped after water leakage is observed at the bottom outlet, thus marking the end of the testing phase.

2.4. Numerical simulations setup

An adequate material model that captures the eutectic bismuth-tin alloy mechanical behavior is necessary to carry out the numerical simulations. Such a model must include the effects of expansion upon solidification, creep, and aging, as discussed before. This model has been presented and described thoroughly in [Hmadeh et al. \(2024b\)](#); & [Jaculli et al. n.d.](#), which also include some example applications. Here, we summarize the key points:

- Expansion upon solidification: this effect is incorporated into the thermal strain by changing the zero-thermal-strain reference temperature of the alloy from 20°C to -150.2°C . This means that the strain at the melting point will be larger, incorporating both the

expansion due to the phase change as well as the existing thermal strain due to temperature changes in the solid phase. Furthermore, we scale down the total expansion due to the solidification depending on how much time has passed since the alloy solidified. The value of -150.2°C is equivalent to a long (infinite) time; for shorter curing times, we obtain different reference temperatures: -101.2°C for 96 hours and -87.3°C for 24 hours. These are the same curing times used in the laboratory tests. An important simplification is that the expansion happens instantaneously in our model (through modification of the reference temperature), but in practice the alloy keeps expanding over time.

- Creep: this phenomenon is modeled through the Anand material model, which accounts for creep behavior and plasticity. This material model is readily available in commercial software such as Ansys. Model parameters for the eutectic bismuth-tin alloy are taken from [Haq et al. \(2021\)](#).
- Aging: no works address the combined effects of load, temperature, and time; thus, the degradation of elastic properties is modeled using the data presented in [Table 2](#).

The numerical simulations are intended to reproduce the push-out tests performed in the laboratory as close as possible to the same conditions. Finite element analysis is employed by using the commercial software Ansys. We reconstruct the geometry presented in [Fig. 1](#), meshing it and ensuring that we provide more elements along the contact surface between the plug outer surface and the pipe inner wall. The pipe ends are fixed to constrain the geometry in terms of rigid body motion. The pressure load from the push-out test is applied to the top surface of the plug, while having an elastic support of negligible stiffness at the bottom surface to also constrain rigid body motion. The pressure is steadily increased to simulate the laboratory push-out test, eventually causing the plug to move downwards. The plug seal is deemed to be broken when the plug is displaced significantly, which is easily observed

on a pressure-displacement plot. Before the numerical push-out test starts, however, the plug is left to cure at the same 4 MPa and curing times as done in the laboratory, intending to capture the creep and aging phenomena. The curing times used in the simulations are 24 and 96 h, while the curing temperatures used are 23 °C, 60 °C, 70 °C, 80 °C, 90 °C, and 120 °C. As aforementioned, the amount of alloy expansion is adjusted according to each curing time.

An important aspect of this problem is the friction between the plug outer surface and the pipe inner wall. Since there is no chemical bond between the two metals, the adherence is purely due to the friction associated with the contact between these two surfaces. The friction coefficient, however, is unknown at this point. We are interested in choosing a value that leads to a hydraulic shear bond strength that matches the results obtained in the laboratory tests. Thus, there is some iterative process testing different values. Ansys is capable of modeling this contact region as a frictional contact, which means that sliding and separation in the normal direction are permitted. The frictional contact type is modeled using the Coulomb friction model and does not discern between static and dynamic friction coefficients, thus allowing only one input, which we calibrate as explained above. A typical value for a dry metal-to-metal seal is 0.3 (Blau, 2008). However, comparisons between preliminary simulation results and the experiments indicated that this coefficient was too high; a lower value should be used, indicating that the seal is not dry, but has a thin film of fluid instead. This is corroborated by experimental observations, in which wet surfaces were observed at the contact when the plug was removed from the pipe for inspection. New simulations were run for friction coefficients in the range of 0.05–0.15, and a value of 0.12 provided a good fit after some iterations, as shown in the results section. Such a value can naturally be refined further.

3. Results and discussion

3.1. Laboratory tests

The hydraulic shear bond strength of the alloy-pipe samples is computed from the peak of each hydraulic pressure-time curve generated for each sample. For each curing temperature, we extract four data points depicting four plug samples tested at the chosen curing times. These are then plotted in Fig. 3 and the values are also tabulated in

Table 5

–Tabulated results of the hydraulic shear bond strength, in bar, for 121 mm long bismuth alloy plugs as a function of curing temperature and curing time (in hours).

| Temp (°C) | Curing time (h) | | | |
|-----------|-----------------|-----|--------------------|-----|
| | 24 | 48 | 72 | 96 |
| 23 | 98 | 100 | 108 | 115 |
| 40 | 97 | 99 | 106 | 112 |
| 60 | 86 | 89 | 90 | 90 |
| 70 | 82 | 76 | 70 | 67 |
| 80 | 70 | 63 | 59 | 56 |
| 90 | 64 | 61 | 55 | 51 |
| 120 | 52 | 50 | <40 (failed @66 h) | |

Table 5. In total, 28 samples (7 curing temperatures x 4 curing times) were prepared and tested. It is important to note that the plugs cured at 120 °C @ 72 h and 120 °C @ 96 h failed during the curing phase, indicating that their hydraulic shear bond strength is below the curing pressure of 40 bar. This was observed at 66 h and is marked in Fig. 3 and Table 5 accordingly. More details of these premature failures are discussed further in the text.

Fig. 3 shows 7 curves representing the hydraulic shear bond strength of 121 mm bismuth alloy plug samples as a function of different curing temperatures and curing times. The upward trajectory observed in the trendlines at both 23 °C and 40 °C indicates a consistent pattern of increasing shear bond strength for the plug as a function of longer curing times. This indicates the alloy plug demonstrates an improved sealing effect over time. This phenomenon is linked to a distinctive characteristic of bismuth alloys, namely the expansion upon solidification. This behavior aligns with findings from Hmadeh et al. (2023a), in which the effect of curing time was studied on bismuth alloy plugs that were set under atmospheric pressure. Furthermore, it was observed that more shear bond strength is built in the initial stages of curing, which is further corroborated by manufacturer data. Fig. 4 illustrates the expansion phenomena and confirms that the rate of expansion for MCP-137 bismuth alloy plugs decreases with time, forming a plateau after 1 month of curing. The numbers presented in Fig. 4 are plotted based on the material properties sheet provided by our bismuth supplier (5N Inc, 2012).

The trendline at 60 °C (Fig. 3) showed a distinct trend in which the

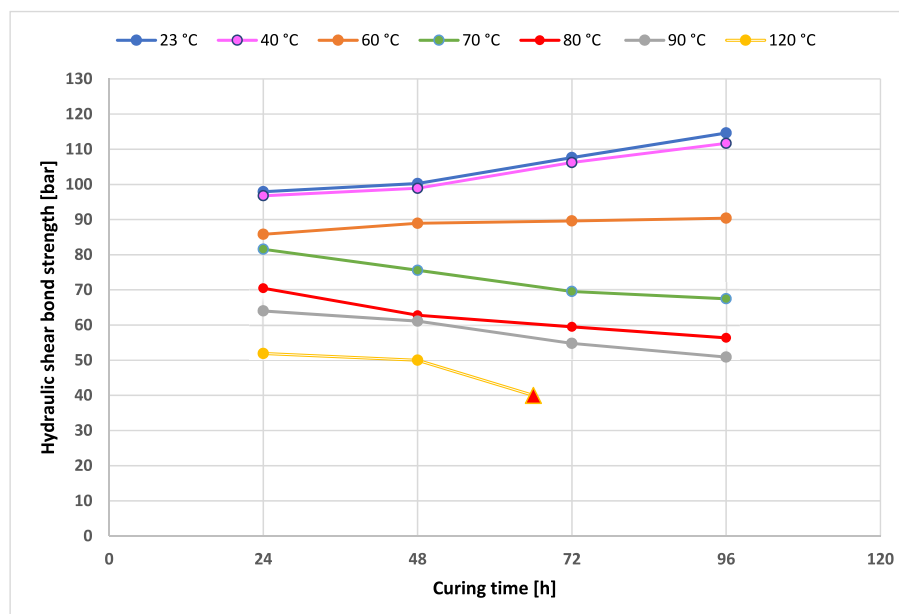


Fig. 3. The variation of hydraulic shear bond strength for 121 mm long bismuth alloy plugs as a function of curing temperature and curing time.

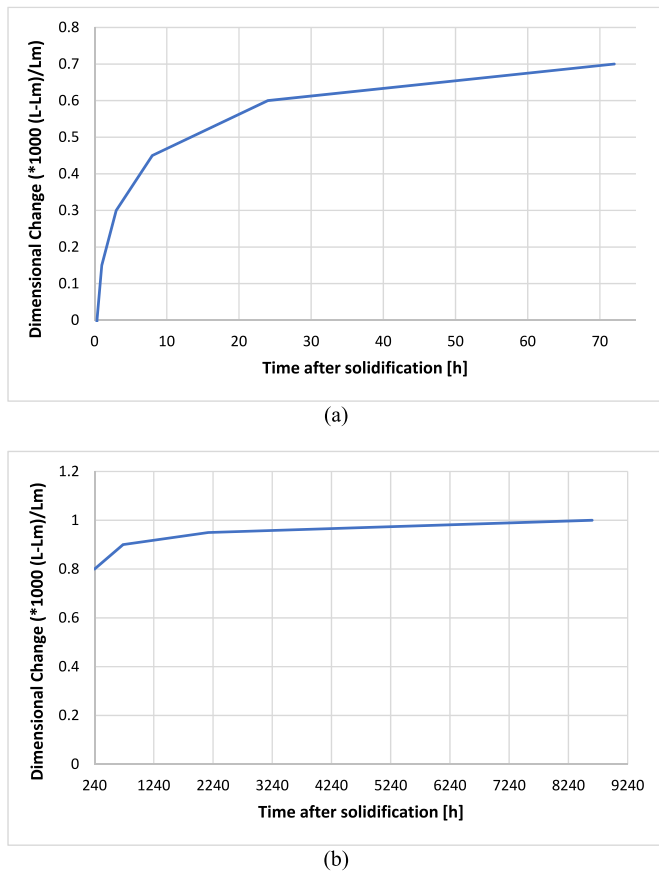


Fig. 4. Growth and shrinkage of an MCP-137 bismuth alloy plug as a function of curing time: (a) from 2 min up to 8 days of curing time; (b) from 10 days up to 12 months (adapted from 5N Inc, 2012).

plug managed to build a negligible shear bond strength of 3 bara between 24 and 48 h. Subsequently, tests at 72 and 96 h of curing time demonstrated a lack of further increase in shear bond strength, plateauing at approximately 89 bar. To gain a more comprehensive understanding of this behavior, it was crucial to observe and analyze how the plug would perform at a higher temperature (e.g., 70 °C). At 70 °C, the hydraulic shear bond strength of the plug sample after 24 h of curing resembled that of the sample tested at 60 °C after 24 h of curing (approximately 80.5 bar). However, with prolonged curing time, indicating an extended exposure of the plug to temperature, an opposing trend was observed. The plug exhibited a decline in shear bond strength, reaching 67.47 bar after 96 h of curing. The authors attribute the comprehensibility of the trendline at 60 °C to it being perceived as the linear boundary distinguishing the diverging trends in hydraulic shear bond strength for a 121 mm bismuth alloy plug. In simpler terms, it is believed that at curing temperatures lower than 60 °C, the metal plug is expected to enhance its shear bond strength over time. Conversely, at temperatures surpassing 60 °C, the plug is anticipated to experience a decline in shear bond strength over time due to the creep phenomenon. This pattern was observed consistently at 70 °C, 80 °C, 90 °C, and 120 °C, in which all four trendlines exhibited a similar negative trend over time, with lower shear bond strength values being attained as the curing temperatures increased toward the melting point. Fig. 5 illustrates this decay for a curing time of 24 h.

As the test temperatures approached the melting point of the alloy, the shear bond strength deteriorated. The lowest shear bond strength values were witnessed at 120 °C, 18 °C below the melting point, in which the plug samples developed a shear bond strength starting with 52 bar after 24 h of curing. Two plug specimens were scheduled for testing after 72 and 96 h, but both experienced failure simultaneously

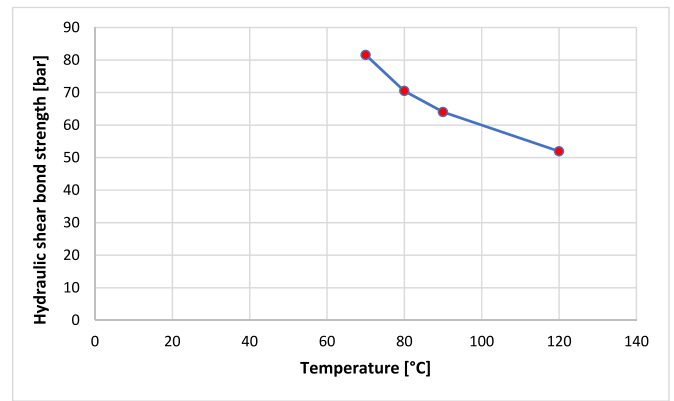


Fig. 5. The variation in shear bond strength for four plug samples allowed to cure for 24 h as a function of increasing temperature.

after 66 h of curing at the initially set pressure of 40 bara. This suggests a likely decline in the shear bond strength of the plug to a level less than or close to 40 bar, consequently leading to its premature failure. In these cases, water leakage was also witnessed from the bottom outlet of the test cell, further indicating the premature failure. The simultaneous failure of both plugs indicates that the conducted test was indeed reliable.

Creep effects become more evident at high temperatures close to the melting point of the alloy, and these effects were indeed witnessed throughout this study. As the curing temperature (120 °C) approaches the melting point (138 °C), the alloy remains solid due to being a eutectic material, but its elastic properties decrease sharply as observed from the material properties. Consequently, the alloy becomes much more deformable, mimicking a fluid-like behavior instead of the one from an actual solid. In addition, creep is time-dependent, which means that it becomes more pronounced over longer exposure times at elevated temperatures. This was confirmed with the last two samples cured at 120 °C which failed to reach 72 h and 96 h of curing.

In this study, various potential variables could have influenced the outcomes, and it is crucial to acknowledge them.

1. Stress level: throughout our experiments, we consistently applied a pressure of 40 bar on the plug. It is important to note that higher stress levels can expedite the creep phenomenon. Therefore, if the experiments were conducted under reduced pressure, we would expect the creep effects to be less pronounced as the temperature rises.
2. Long-term deformation effects: the tendency of bismuth-tin alloys to creep, or slowly deform, is more evident when they are subjected to high temperatures for extended periods. Therefore, if the experiments had continued for longer than 96 h, it is likely that the 121 mm plugs would have failed at temperatures of 70, 80, and 90 °C due to the observed negative trend. According to Fig. 6, these failures would occur approximately after 9.5, 7.5, and 6.25 days, respectively (marked by the yellow Xs) under the aforementioned testing conditions.
3. Grain structure and composition: the tendency of an alloy to gradually creep under constant stress is affected by its grain structure and the elements that make up its composition (Guangyin et al., 2001). Various additives, impurities, and microscopic structural characteristics in the alloy play a significant role in determining its behavior when subjected to high temperatures and stress. Normally, fine-grained materials often exhibit better creep resistance than coarse-grained ones.
4. Creep rate: creep is often characterized by its creep rate. Creep rate is a key characteristic representing the speed of deformation over time under unchanging stress and high temperature and is typically

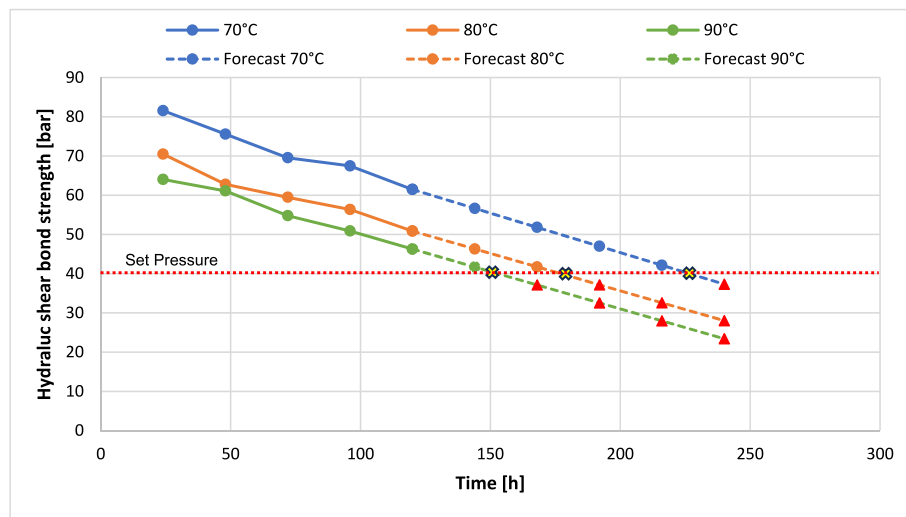


Fig. 6. Predicted trends in hydraulic pressure at temperatures of 70, 80, and 90 °C. Yellow Xs represent the predicted time at which the plug would fail.

measured to understand its effect on the results. However, in our case, it was not possible to measure the creep rate due to the lack of required equipment. This rate can differ greatly depending on the particular composition of the alloy and the conditions it is subjected to. This variable is planned to be addressed in future work.

- Pipe roughness: the creep behavior could be severely affected by the roughness of the pipe where a rougher pipe could potentially lead to an increased friction, thereby providing more resistance to the alloy to creep under prevailing stress conditions. However, this roughness might have a negative effect by introducing points of stress concentration (Wen et al., 2016). Such stress concentrations are likely to accelerate creep deformation in those localized areas, potentially leading to non-uniform creep behavior across the seal. In other words, pipe roughness might either facilitate or hinder creep mechanisms thus requiring a thorough investigation.

Eutectic bismuth tin alloys will always face significant challenges under prolonged exposure to high temperatures. The key issue is determining the feasibility of using these low melting point alloys at such temperatures. The solution is not a universal, “one-size-fits-all” alloy suitable for every wellbore. Rather, the approach involves tailoring the alloy to suit the specific conditions of each well. This means we need to carefully consider, and pre-plan the composition and properties of the alloy plug based on the depth and environmental conditions it will be installed in.

During the initial stages of planning, other potential alloys like bismuth-tin-antimony and bismuth-silver could be considered due to their enhanced sealing performance and creep resistance (Bosma et al., 2010; Oluleke and Eden, 2021). A small addition of antimony is capable of improving creep resistance, increasing the solidification rate, reducing the risk of liquid metal embrittlement, hindering the leach of tin from the alloy, and increasing the corrosion resistance. Thus, can be used in deeper wells where pressures are usually higher. Similarly, adding silver to bismuth exhibits an improved creep, decreased risk of liquid metal embrittlement, high degree of corrosion resistance, and much better mechanical properties in terms of tensile stress, ultimate tensile strength, and volumetric expansion. BiAg can perform at high temperatures in which other alloys would melt. However, it is important to have bismuth in higher percentages to retain the expansion property, as added silver increases the ductility and strength, but also reduces the melting point (as cited in Hmadeh et al., 2024a). Thus, when designing a bismuth alloy, there is a trade-off between decreasing its melting point (for easier placement inside the well) and losing expansibility (a property that is desired).

3.2. Numerical simulations

Fig. 7 presents the plug bottom displacement as a function of the increasing differential pressure applied on top, for the six chosen curing temperatures and a curing time of 24 h, while Fig. 8 presents the same but for a curing time of 96 h. We see that, as the pressure builds up, there is a sudden increase in plug displacement, indicating that the plug seal has been breached. We then collect the pressure values at which this happens, meaning that they will be the numerical values of the hydraulic shear bond strength. This is similar to how we collected the peaks from the test curves to determine the hydraulic shear bond strength in the laboratory.

The collected results are combined and presented in Fig. 9. It is observed that the resisted pressure, i.e. the pressure at which the seal breaks, decreases as the curing temperature rises for the same curing duration. Similarly, this resisted pressure decreases with longer curing times at a consistent curing temperature. Although higher temperatures facilitate greater creep, enhancing the adhesion between the plug and the inner surface of the pipe, there is a significant decline in the elastic properties with temperature increase, as demonstrated in Table 2. Therefore, improved adhesion does not offset the negative effect that elevated temperature has on the elastic properties of the alloy. Consequently, the plugs become weaker with elevated temperatures, which has been also witnessed throughout the laboratory tests conducted.

Better visualization is achieved if we combine the results from Figs. 3 and 9 into a single plot, as seen in Fig. 10. Comparison have shown good agreement for higher temperatures, indicating the same downwards trend from the experiments. Whereas, at lower temperatures, an upwards trend should have been witnessed instead, but the numerical results also had a downwards trend for them. According to the experimental results from the previously described setup, there seems to be a threshold temperature around 60 °C, in which the expansion and creep effects cancel each other, indicated by the constant trend over time. Above 60 °C, the creep effect seems to be more predominant, while the expansion effect is more relevant below this temperature. Since good agreement was achieved for the higher temperatures, it implies that the Anand plasticity model is capable of capturing the creep + viscoplastic behavior of this alloy. However, disagreement between the experimental and simulation results at lower temperatures means that the mechanism that strengthens the plug over time is not captured adequately in the material model. Therefore, due to this discrepancy between experimental and simulations results for the temperatures 23 °C, 40 °C, and 60 °C, the numerical results for these temperatures have been omitted from the graph.

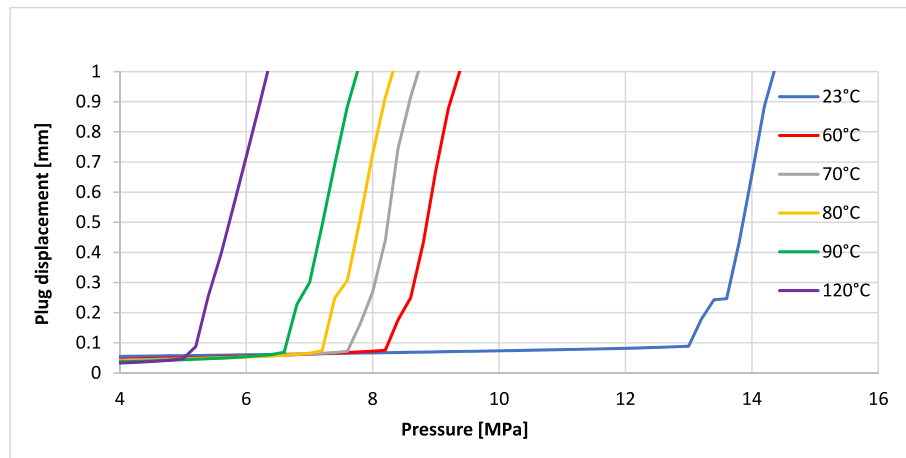


Fig. 7. Plug bottom displacement as a function of the applied pressure differential on top, for different curing temperatures and a curing time of 24 h.

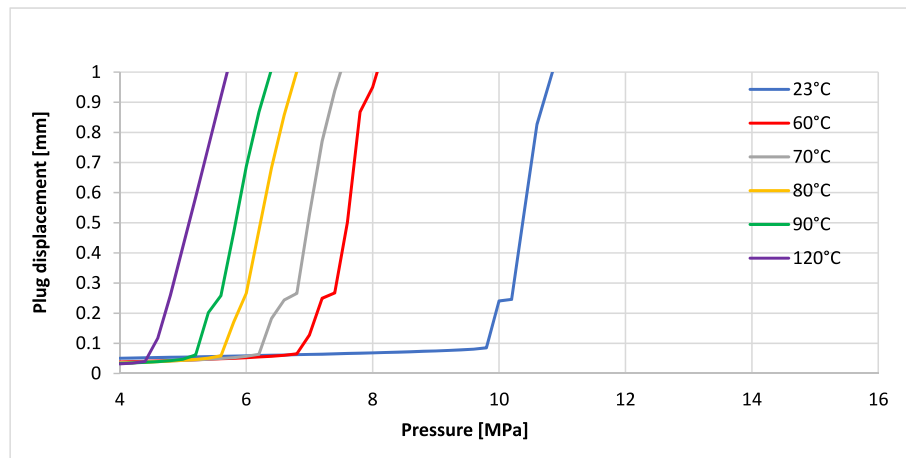


Fig. 8. Plug bottom displacement as a function of the applied pressure differential on top, for different curing temperatures and a curing time of 96 h.

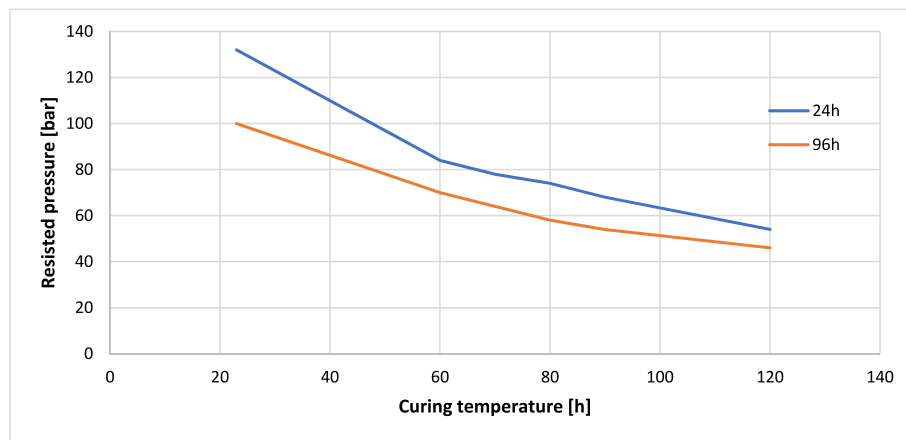


Fig. 9. Resisted pressure as a function of curing temperature for curing times of 24h and 96h.

One important simplification made in the material model is that the expansion upon solidification happens over time in practice but was modeled as happening instantaneously. This approach has been followed in similar problems such as cement shrinkage (Lavrov et al., 2019). This assumption was necessary to accommodate the bismuth behavior within the Anand plasticity model available in the software. Therefore, the discrepancy in trends for 23 °C, 40 °C, and 60 °C could be

a consequence of this hypothesis, which needs further improvements in the model. Nevertheless, important modeling steps have been discussed and should guide initial simulations due to the lack of other existing literature regarding this alloy in this particular application.

Furthermore, we note that the plug at 120 °C failed in the laboratory tests before even reaching 96 h, while the numerical model had yet to fail at 96 h – although the downward trend indicates that it would fail

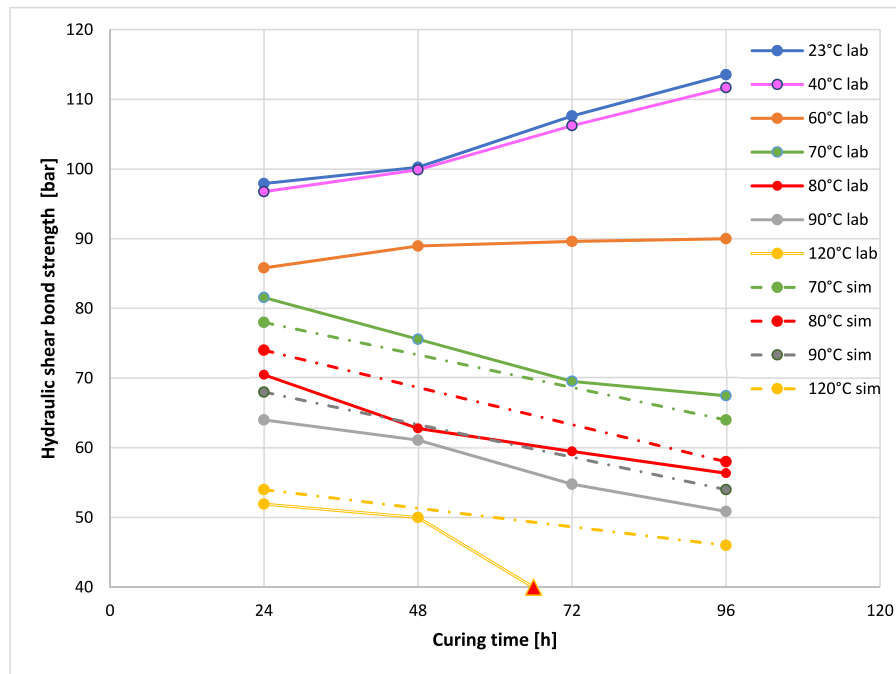


Fig. 10. Comparison of the plug performance as evaluated by laboratory tests and numerical simulations.

eventually. The slope of the simulation curve captures the slope of the laboratory curve between 24 and 48 h, but then there is a sharp drop in the laboratory results that is not seen in the simulation. This is a limitation in the Anand plasticity model as it models up to the secondary creep stage and does not incorporate accelerated failure caused by tertiary creep, which is the phenomenon that has this abrupt behavior. Instead, in this model, the alloy would remain creeping at the secondary stage until eventually it would not withstand the initial curing pressure of 40 bar but at a longer curing time.

4. Conclusions

The primary objective of our research was to evaluate the performance of eutectic bismuth alloy plugs under various temperatures and curing durations. Our small-scale laboratory investigation yielded several insights:

- Below 60 °C, we observed an improvement in the shear bond strength of the metal plug over time, suggesting enhanced bonding capabilities at lower temperatures.
- Above 60 °C, there was a noticeable reduction in shear bond strength over time, attributed to the creep phenomenon.
- Creep effects become more evident at high temperatures close to the melting point of the alloy. As the curing temperature of 120 °C approaches the melting point of the alloy (138 °C), the shear bond strength deteriorates drastically.
- Several factors could have impacted these results, including stress levels, long-term deformation, the grain structure and composition of the alloy, creep rates, and the roughness of the pipe.
- Results from the developed numerical model have shown a good agreement with the obtained laboratory test results for higher curing temperatures while indicating different trends for lower curing temperatures, implying that further model refinements are necessary, especially in the assumption of instantaneous expansion and simplifications in the creep behavior. Nevertheless, a groundwork for simulations was laid and should guide further work.

Eutectic bismuth tin alloys will always face challenges under

prolonged exposure to high temperatures. The solution is not a universal, “one-size-fits-all” alloy suitable for every wellbore but rather a tailored approach, customizing the alloy’s composition and properties to fit the specific conditions of each well. This necessitates a strategic pre-planning phase to determine the most suitable alloy composition for the intended wellbore environment and depth the plug will be installed in.

CRedit authorship contribution statement

Lewaa Hmadeh: Writing – review & editing, Writing – original draft, Visualization, Methodology, Investigation, Formal analysis, Conceptualization. **Marcelo Anuniação Jaculli:** Writing – review & editing, Writing – original draft, Validation, Software, Formal analysis, Conceptualization. **Noralf Vedvik:** Resources. **Behzad Elahifar:** Writing – review & editing, Supervision. **Sigbjørn Sangesland:** Writing – review & editing, Supervision, Project administration, Funding acquisition.

Declaration of competing interest

The authors declare the following financial interests/personal relationships which may be considered as potential competing interests: Lewaa Hmadeh reports financial support was provided by Research Council of Norway. Marcelo Anuniação Jaculli reports financial support was provided by Research Council of Norway. If there are other authors, they declare that they have no known competing financial interests or personal relationships that could have appeared to influence the work reported in this paper.

Data availability

The authors do not have permission to share data.

Acknowledgements

The authors acknowledge the Research Council of Norway (RCN) for financing the Center for Research-based Innovations "SWIPA - Center for Subsurface Well Integrity, Plugging and Abandonment", RCN project no.

309646, for which the work has been carried out. The center is also financed by the operating companies AkerBP, Equinor ASA and Wintershall Dea Norway, and includes in addition more than 20 in-kind contributing industry partners. The R&D partners in SWIPA are SINTEF, NORCE, IFE, NTNU and UIS.

References

- Blau, P.J., 2008. Friction Science and Technology from Concepts to Applications, second ed. CRC Press. <https://doi.org/10.1201/9781420054101>.
- Bosma, M.G.R., Cornelissen, E.K., Dimitriadis, K., Worrall, R.N., 2010. *Creating a Well Abandonment Plug* (Patent US7640965B2). United States Patent.
- Carragher, P., Fulks, J., 2018. Well abandonment solutions utilizing bismuth and thermite. In: Abu Dhabi International Petroleum Exhibition & Conference. <https://doi.org/10.2118/193118-MS>.
- Carter, L.G., Evans, G.W., 1964. A study of cement-pipe bonding. J. Petrol. Technol. 16 (2), 157–160. <https://doi.org/10.2118/764-PA>.
- Fulks, J., Carragher, P., Tools, B.O., 2021. SPE-204404-MS squeezing perforations rigless-No pumping or injection required. In: <http://onepetro.org/SPECTWI/proceedings-pdf/21CTWI/1-21CTWI/D011S001R002/2435502/spe-204404-ms.pdf/1>.
- Guangyin, Y., Yangshan, S., Wenjiang, D., 2001. Effects of bismuth and antimony additions on the microstructure and mechanical properties of AZ91 magnesium alloy. www.elsevier.com/locate/msea.
- Haq, M.A., Hoque, M.A., Suhling, J.C., Lall, P., 2021. Anand parameters for eutectic tin-bismuth solder. InterSociety Conference on Thermal and Thermomechanical Phenomena in Electronic Systems. ITherm, 2021-June, pp. 926–932. <https://doi.org/10.1109/ITherm51669.2021.9503292>.
- Hmadeh, L., Elahifar, B., Sangesland, S., 2023a. The sealing behavior of bismuth-based metal plugs. In: Proceedings of the ASME 2023 42nd International Conference on Ocean, 9. Offshore and Arctic Engineering. <https://doi.org/10.1115/OMAE2023-104309>. *Offshore Geotechnics; Petroleum Technology*.
- Hmadeh, L., Elahifar, B., Sangesland, S., Abrahamsen, A.E., 2023b. A full laboratory study on the physical and mechanical properties of a bismuth plug. SPE - International Association of Drilling Contractors Drilling Conference Proceedings. <https://doi.org/10.2118/212561-MS>.
- Hmadeh, L., Anunciação Jaculli, M., Elahifar, B., Sangesland, S., 2024a. Development of bismuth-based solutions for well plugging and abandonment: A review. Petroleum Research 9 (2), 250–264. <https://doi.org/10.1016/j.ptlrs.2024.01.003>. <https://doi.org/10.1016/j.ptlrs.2024.01.003>. KeAi Publishing Communications Ltd.
- Hmadeh, L., Manataki, A., Jaculli, M., Elahifar, B., Sangesland, S., 2024b. A Sealability Study on Bismuth-Tin Alloys for Plugging and Abandonment of Wells. SPE J. 29 (2024), 3500–3515. <https://doi.org/10.2118/219744-PA>.
- Jaculli, M. A., Hmadeh, L., Sangesland, S., & Elahifar, B. (n.d.). Numerical modeling of bismuth-based plugs for well plug and abandonment. Proceedings of the ASME 2024 43rd International Conference on Ocean, Offshore and Arctic Engineering. Manuscript Accepted.
- Knutsen, T., 2019. A novel approach to qualifying bismuth as a barrier material. University of Stavanger. <https://uis.brage.unit.no/uis-xmlui/handle/11250/2621291>.
- Lavrov, A., Bhuiyan, M., Stroisz, A., 2019. Push-out test: why bother? J. Petrol. Sci. Eng. 172, 297–302. <https://doi.org/10.1016/j.petrol.2018.09.067>.
- Manataki, A., Kontis, P., Sangesland, S., 2023. Investigation of the microstructure of bismuth alloy and its interaction with cement and steel casing. In: Proceedings of the ASME 2023 42nd International Conference on Ocean, 9. Offshore and Arctic Engineering. <https://doi.org/10.1115/OMAE2023-103843>. *Offshore Geotechnics; Petroleum Technology*.
- N Inc., 2012. Product Data Sheet MCP 137/Metspec 281 Alloy. www.5nplus.com.
- Oluleke, J., Eden, R., 2021. Improved Well Sealing Material and Method of Producing a Plug. UK Patent.
- Stoll, C., 2017. Facts About Bismuth. <https://www.livescience.com/39451-bismuth.html>.
- Wen, S., Zhou, S., Liu, X., 2016. Effect of surface roughness on the determination of the creep properties of material by using three points bending creep test. <https://doi.org/10.2991/ismems-16.2016.5>.
- Yang, H., Fu, Q., Wu, J., Qu, L., Xiong, D., Liu, Y., 2020. Experimental study of shear and hydraulic bonding strength between casing and cement under complex temperature and pressure conditions. R. Soc. Open Sci. 7 (4), 192115 <https://doi.org/10.1098/rsos.192115>.
- Zhang, H., Ramakrishnan, T.S., Elias, Q.K., Perez, A., 2020. Evaluation of bismuth-tin alloy for well plug and abandonment. SPE Prod. Oper. 35 (1), 111–124. <https://doi.org/10.2118/199363-PA>.
- Zhang, H., Ramakrishnan, T.S., Elkady, Y.M., Feng, Y., Elias, Q.K., 2021. Comparative evaluation of bismuth-silver and bismuth-tin alloys for plug and abandonment. SPE Drill. Complet. 36 (2), 368–382. <https://doi.org/10.2118/202488-PA>.
- Zhang, H., Ramakrishnan, T.S., Elias, Q.K., 2022. Testing low-melting-point alloy plug in model brine-filled wells. SPE Prod. Oper. 37 (1), 9–16. <https://doi.org/10.2118/205001-PA>.